International Journal of Fatigue 35 (2012) 31–36

Contents lists available at ScienceDirect

International Journal of Fatigue

journal homepage: www.elsevier.com/locate/ijfatigue

Effects of thermal exposure on cyclic deformation and fracture behavior of Ti600 titanium alloy

T. Yu [a], L. Wang [a,*], Y.Q. Zhao [b], Y. Liu [a]

[a] Key Laboratory for Anisotropy and Texture of Materials (Ministry of Education), Northeastern University, Shenyang 110004, China
[b] Northwest Institute for Nonferrous Metal Research, Xi'an 710016, China

ARTICLE INFO

Article history:
Received 9 May 2010
Received in revised form 18 November 2010
Accepted 29 December 2010
Available online 1 January 2011

Keywords:
Ti600 titanium alloy
Cyclic deformation behavior
Fracture behavior
Thermal exposure
Cyclic stress response

ABSTRACT

Effects of thermal exposure on cyclic deformation and fracture behavior of Ti600 alloy were investigated by laser scanning confocal microscope (LSCM), scanning electron microscope (SEM) and transmission electron microscope (TEM). The results demonstrated that both the nonthermal exposure (NTE) specimens and the thermal exposure (TE) specimens showed the cyclic softening, within a total strain amplitude range from ±0.45% to ±1.00%. During thermal exposure, since the harder α_2 (Ti_3Al) phase precipitated in the α_p (primary α) phase, the resistance of crack propagation of α_p phase could be increased by the precipitation of α_2 phase. Therefore, the fracture behavior of TE specimens is different with that of NTE specimens. For the NTE and TE specimens, the crack mainly passes through the α_p phase with "cutting" and "bypass", respectively.

1. Introduction

For aircraft and space applications, a strong demand exists for materials with low density and high strength. In jet engines, materials must also be resistant against high temperature. Titanium alloys are important materials for such applications, because of their low density and excellent mechanical properties, in particular at elevated temperature. Recent years, with the requirement of aircraft construction integrity, reliability and durability, high temperature titanium alloy which can be serviced for long times and stably at 600 °C, have been explored competitively all over the world, for instance, Ti-1100 (US), IMI834 (UK), BT18Y and BT36 (Russia), Ti60 and Ti600 (China) [1–6].

Ti600 alloy is a near-α high temperature titanium alloy to be used at 600 °C, and is developed for service in applications such as blades and turbine disks which are subjected to complicated loading at high temperatures. Ti600 alloy was obtained by adding rare earth element Y to Ti-1100 alloy [7]. Ti600 alloy has excellent tensile strength, creep resistance and stress rupture properties [7–11]. In previous reports, a lot of studies were concentrated on types of microstructure, creep properties, tensile properties, and so on. However, the study on cyclic deformation and fracture behavior of Ti600 alloy before and after thermal exposure has not been reported. It is well known that fatigue processes are combined with the cyclic deformation, crack initiation and crack propagation [12]. It is very necessary to clear the microstructural changes and fracture behavior under the cyclic loading for the well understanding of fatigue behavior of Ti600 alloy.

Based on the above background, the effects of thermal exposure on cyclic deformation and fracture behavior of Ti600 alloy were investigated in the present research, especially the cyclic stress response characteristics to straining, crack initiation behavior and crack propagation behavior.

2. Material and experimental procedures

2.1. Material and specimen

Ti600 alloy used in present research was prepared by melting in vacuum consumable electrode arc furnace for three times. After casting, the ingots were forged and hot rolled (in ($\alpha + \beta$) dual-phase region) into round bar with a diameter of 12 mm. The chemical compositions of Ti600 alloy is shown in Table 1. The β transus temperature (T_β) of Ti600 alloy was 1010 °C.

When Ti600 alloy solution treated below T_β and aged subsequently, it has bi-modal microstructure (as shown in Fig. 1). From Fig. 1, bi-modal consisting of equiaxed primary α phase (α_p) in a lamellar $\alpha + \beta$ matrix (transformed β phase, β_T), for which the volume fraction of α_p phase is about 20%, and average grain size of the α_p phase is about 15 μm.

In order to estimate the microstructure stability of Ti600 alloy at 600 °C, thermal exposure was carried out at 600 °C after solution

* Corresponding author. Tel.: +86 24 83687725; fax: +86 24 23906316.
E-mail address: wanglei@mail.neu.edu.cn (L. Wang).

0142-1123/$ - see front matter © 2011 Elsevier Ltd. All rights reserved.
doi:10.1016/j.ijfatigue.2010.12.015

Table 1
Chemical composition of Ti600 alloy (mass%).

Al	Sn	Zr	Mo	Si	Y	Ti
6.0	2.8	4.0	0.5	0.4	0.1	Bal.

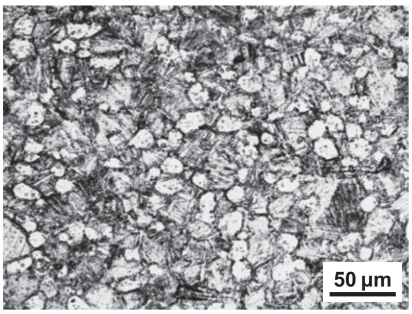

Fig. 1. Microstructures of Ti600 alloy (1005 °C/2 h, AC + 650 °C/8 h, AC).

treatment and aging treatment. The detailed heat treatments are shown as follows:

- NTE: 1005 °C/2 h, AC + 650 °C/8 h, AC
- TE: NTE + 600 °C/100 h, AC

The schematic illustration of cyclic deformation specimen is shown in the Fig. 2. The cyclic deformation specimen in a round bar-shaped with gauge sections of $\Phi 6\,mm \times 21\,mm$ following ASTM recommendations (ASTM E606-98), were machined after heat treatment. The specimen axis was parallel to the rolling direction. In order to avoid the influence of geometric discontinuity and surface condition on the experimental results, the surface of uniform-gauge sections of the specimens were manually polished carefully before testing.

2.2. Testing procedures

The cyclic deformation tests were carried out with an electro-hydraulic fatigue testing machine model MTS-810 at room temperature and the cyclic loading direction was parallel to the specimen axis. An extensometer with a gauge length of 15 mm for strain measurement was attached to the specimen. Cyclic deformation tests were performed under fully reversed axial total strain control using a sine wave at a strain ratio of $R_\varepsilon = -1$. The cyclic straining of the specimen started with the tensile loading. The loading frequency in the present study was kept to be constant at 0.1 Hz for various total strain amplitudes.

2.3. Microstructural analysis

The microstructures, gauge section surface morphologies and fracture surfaces of the cyclic deformation specimens were examined by both LSCM (model OLYMPUS-OLS3100) and SEM (model JEOL JSM-7001F). Precipitates were analyzed by TEM (model TECNAI G^2 20).

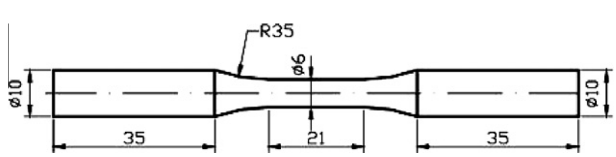

Fig. 2. Schematic illustration of cyclic deformation specimen (in mm).

3. Results and discussion

3.1. Microstructure evolutions of Ti600 alloy during thermal exposure

It is well known that the α_2 phase usually precipitated during long-term aging or thermal exposure, which mainly formed in the α_p phase because the Al is always rich in the α_p phase [13–15]. In the present research, the precipitates of α_2 phase can only be found in the TE specimens, as shown in Fig. 3. The α_2 phase is white particle with size of about 5–20 nm, as shown in Fig. 3a. The selected-area diffraction pattern (SAD) is shown in Fig. 3b.

Because of the α_2 phase precipitated from α_p phase after thermal exposure, the hardness of α_p phase has been changed from 357 HV to 386 HV. That is to say that after thermal exposure the hardness of α_p phase is increased about 8.1%, the α_2 phase is considered as the main reason for the increasing of the hardness of α_p phase.

3.2. Cyclic stress response to straining

Fig. 4 shows the cyclic stress response to straining of the specimens in NTE and TE conditions, respectively. Plotted in the figure are the cyclic stress amplitude vs. the cyclic numbers at different constant total strain ranges, typically being ±0.45%, ±0.50%, ±0.60%, ±0.70%, ±0.80% and ±1.00%. The cyclic stress amplitude was taken as the average of the peak values of the stress in tension and in compression during the cyclic deformation. From the Fig. 4, it can be noticed that there are different degrees of softening at different total strain amplitude weather in the NTE or HE specimens, and both the degree and the rate of softening increase with increasing of total strain amplitude.

Generally, when a material is cyclic strained, the response stress usually shows an increase or a decrease with loading cycles, which are called cyclic hardening or cyclic softening, respectively. For some material it may reach a stage where the stress remained constant after the initial hardening or softening, which is called cyclic saturation [16]. And the cyclic stress response to straining of a material depends on its initial microstructure, serving condition and deformation history [17–19].

In the present study, cyclic softening occurred for both the NTE and TE specimens. This phenomenon may be caused by two factors. First, the decreasing of effective stress caused by slip is higher than the increasing of internal stress. As shown in the Fig. 5, the slip band formed after cyclic deformation in both the NTE and TE specimens, it leads the specimens to exhibit cyclic softening characteristic. Second, since the decreasing of effective area for cyclic stress response caused by the initiation of micro-cracks, cyclic deformation specimens showed cyclic softening. The decreasing of effective area for cyclic stress response is considered as the main reason of cyclic softening, especially for the total strain amplitude higher than ±0.50%.

3.3. Fracture behavior with cyclic loading

3.3.1. Fractography characteristics

The fracture surfaces with different straining amplitude were examined by SEM, as shown in Fig. 6. It was found that cracks initiated at the specimen surface, and it seems no evident differences between NTE specimens and TE specimens on the fracture surface, since free surface was easy to yield and lead to damage during cyclic deformation.

From Fig. 6a and b, it can be divided into “A”, “B” and “C” typical regions, which are the crack initial region, the crack propagation region and the final fracture region, respectively. The crack propagation region exhibited radial smooth facets on which the cyclic